A Single-Site Model for Water: Parameterized for the Reproduction of the Melting Point of Ice I_h

Patrick B. Louden[1] and J. Daniel Gezelter[1]

[1] *Department of Chemistry, University of Notre Dame, Notre Dame, IN 46556*

This report is a living document on the progress of developing a single-site model for water, parameterized to reproduce the experimentally observed melting point of ice I_h.

INTRODUCTION

Abascal and Vega have recently observed that the melting points of common 3-site and 4-site water models correlates strongly with their dipolar and quadrupolar interactions.[1–3] To quantify dipole and quadrupole moments, we must first consider how to define our coordinate system. For planar water models, we define our coordinate system in the following way; the z axis as the dipole moment direction (the HOH bisector), the y axis parrallel to the vector connecting the two Hydrogens, and the x axis normal to the plane of the molecule. This choice of coordinate system follows that of Rick, and thus the equations in his paper follows naturally. Abascal and Vega define their coordinate system by flipping the x and y axes, resulting in a few sign changes between our work and theirs. Having defined a coordinate system, we can calculate the traceless quadrupole tensor, Θ, for any water model by

$$\Theta_{ij} = \frac{1}{2}\sum_{\alpha} q_\alpha (3 r_{i,\alpha} r_{j,\alpha} - |\vec{r_\alpha}|^2 \delta_{ij}) \tag{1}$$

where, q is the charge and the sum is taken over all charged sites in the model. The traceless quadrupole tensor has certain special properties, and is aptly named for one of them; which is the trace, (Tr), of the tensor is null.

$$Tr(\Theta) = \sum_{i,j} \Theta_{ij}\delta_{ij} = 0 \tag{2}$$

While having a traceless tensor can make certain calculations easier to perform, it is also possible to calculate a traced quadrupole tensor Q, one in which the trace is not null.

$$Q_{ij} = \frac{1}{2}\sum_{\alpha} q_\alpha (r_{i,\alpha} - r_{i,com})(r_{j,\alpha} - r_{j,com}) \tag{3}$$

Here, $r_{i,com}$ is the position of the center of mass in the i-th dimension, and therefore the position of the quadrupole moment is set at the center of mass of the molecule. It will be desirable to change between the traceless and traced quadrupole tensors during this work, and changing between the two formalisms can be achieved by the following

$$\Theta = 3Q - Tr(Q) \tag{4}$$

Based on the suggestion of Carnie and Patey[4], as well as Rick[5], Abascal and Vega have described an effective tetrahedral quadrupole moment (Θ_T), defined in ours and Rick's coordinate system for a traceless quadrupole as

$$\Theta_T = \frac{1}{2}(\Theta_{yy} - \Theta_{xx}). \tag{5}$$

Abascal and Vega have shown that the water models which most accurately reproduce the meling point of ice I_h have a ratio of their dipole moment to Θ_T of approximately unity. The equivalent expression for the traced quadrupole tensor is given as

$$Q_T = \frac{3}{2}(Q_{yy} - Q_{xx}). \tag{6}$$

The Q_T values for each of the water models investigated by Abascal and Vega are shown in Table I, along with the non-zero elements of their traced quadrupole tensors.

	Q_{xx}	Q_{yy}	Q_{zz}	$Tr(Q)$	QBar	Q_T	T_m
TIP4P/Ice	0.0	1.6629	0.7427	2.3657	2.8143	2.4348	272.2
TIP4P/2005	0.0	1.531	0.7034	2.2336	2.6553	2.2969	252.1
TIP4P/Ew	0.0	1.4427	0.6617	2.1044	2.5017	2.1640	245.5
TIP4P	0.0	1.4311	0.6584	2.0895	2.4814	2.1466	232.0
SPC/E	0.0	1.357	0.5267	1.8837	2.3700	2.0356	215.0
SPC	0.0	1.3129	0.5095	1.8224	2.2928	1.9693	109.5
TIP3P	0.0	1.1476	0.5337	1.6812	1.9894	1.7214	146

TABLE I: Traced quadrupole tensors for the water models investigated by Abasca and Vega. All elements of the tensors are in units of DÅ , melting temperatures are reported in Kelvin.

In Figures 1 and 2, we have replotted the melting point for ice I_h of these water models by $\overline{Q}$ and the trace of their quadrupole tensor, where $\overline{Q}$ is given by,

$$\overline{Q} = \sqrt{2(3Q : Q - (Tr(Q))^2)} \quad (7)$$

We see in both cases there is a strong correlation between the values of their quadrupole tensors and their melting point.

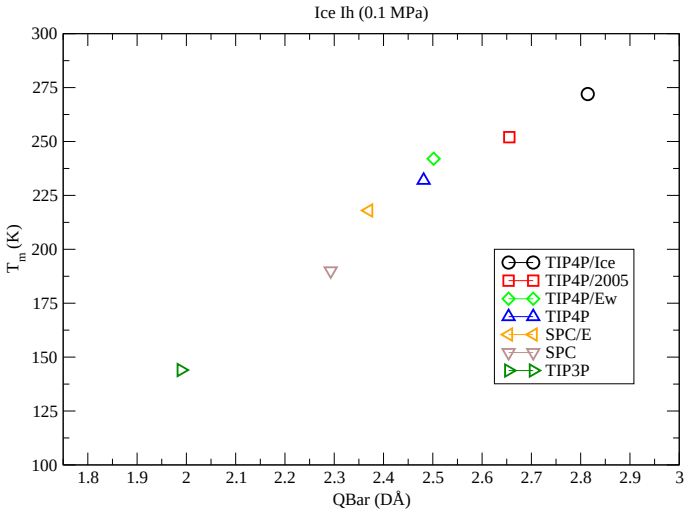

FIG. 1: Melting point for ice I_h of several popular water models as a function of the QBar for the model. We see a strong correlation between a more accurate melting point and a larger value of QBar. We estimate that a QBar of approximately 2.8 DÅwill result in the experimental melting point of 273.15 K. A linear regression of the data resulted in an equation of best fit of $y = 158.89x - 166.83$. From this, we have predicted an optimal QBar to be 2.7690 DÅ .

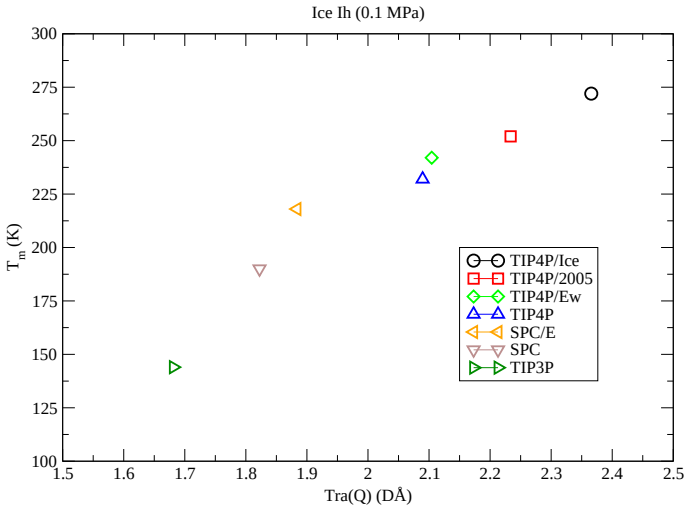

FIG. 2: Melting point for ice I_h of several popular water models as a function of the trace of the quadrupole tensor for the model. We see a strong correlation between a more accurate melting point and a larger value of the trace. We estimate that a trace of approximately 2.3 DÅwill result in the experimental melting point of 273.15 K.

Based on this observation, we have begun work on a 1-site model with intentions of setting the dipole moment and structuring the quadrupole tensor in such a way that will give us a ratio of unity. As a starting point, we have collapsed the 4-site TIP4P-Ice model[6] onto a 1-site model (TIP1P/Ice). The geometric parameters, the Lennard-Jones and charges, and the dipole and quadrupole elements that have value can be found for both models in Table II, Table III, and Table IV respectively.

	OH bond length Å	OM bond length Å	HOH °
TIP4P/Ice	0.9572	0.1577	104.52
TIP1P/Ice	-	-	-

TABLE II: Geometric parameters of the TIP4P/Ice and TIP1P/Ice models.

	σ Å	ϵ kcal/mol	q_H (e)	q_M (e)
TIP4P/Ice	3.1668	0.2108509	0.5897	-1.1794
TIP1P/Ice	3.1668	0.2108509	-	-

TABLE III: Lennard-Jones and charge parameters of the TIP4P/Ice and TIP1P/Ice models.

	μ D	Q_{xx} DÅ	Q_{yy} DÅ	Q_{zz} DÅ	Q_T DÅ
TIP4P/Ice	2.4255966	0.0	1.62291807	0.74278997	2.434
TIP1P/Ice	2.4255966	0.0	1.62291807	0.74278997	2.434

TABLE IV: Dipole and quadrupole parameters for the TIP4P/Ice and TIP1P/Ice models.

TIP1P/ICE

Gas Phase Dimer

This section contains details and graphs of the attempts to tune the TIP1P/Ice model to the experimental and ab initio predicted results for the gas phase water dimer. In order to tune the TIP1P/Ice model, we are going to calculate the geometry of the gas phase water dimer as shown in Figure 3[7].

There are three values of interest for our characterization of the water dimer. The first is the oxygen-oxygen separation distance, R_{OO}. The other two parameters of the dimer are the two angles, θ and ϕ. These angles are taken from the HOH bisector to the R_{OO} vector. While the length of the R_{OO} vector will be dependent on the magnitude of the dipole and quadrupole moments, the relative contributions of Q_{xx}, Q_{yy}, and Q_{zz} will strongly influence the angles. We also expect that the Lennard-Jones parameter σ will strongly influence the magnitude

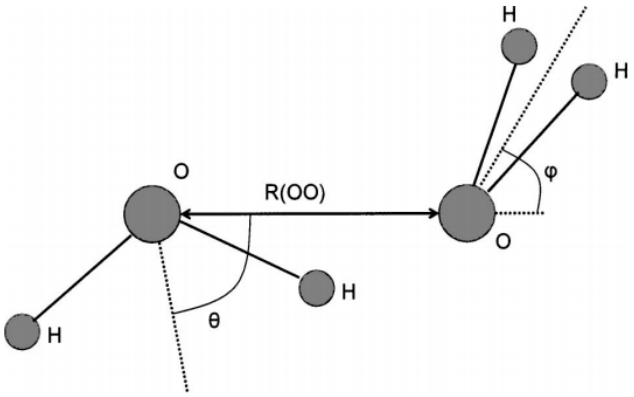

FIG. 2. Definition of the distance $R(OO)$ and the angles θ and ϕ that determine the relative position and orientation of the monomers of the water dimer in the gas phase.

FIG. 3: The gas phase water dimer geometry.

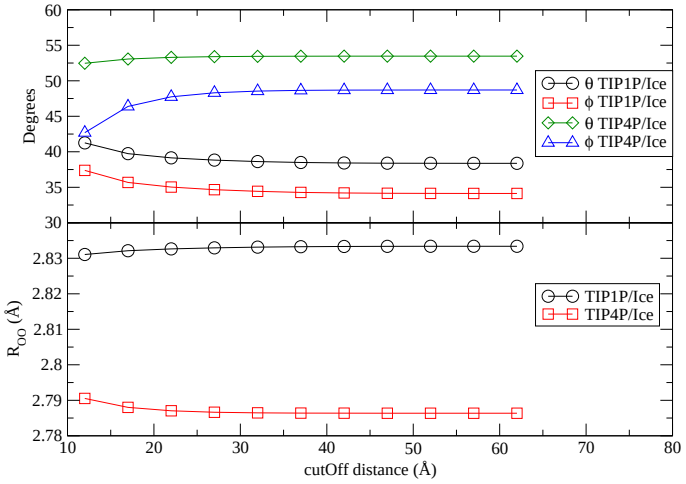

FIG. 4: Damping α set to 0.05 Å^{-1} and the simulation box was $300 \times 300 \times 300$ Å .

of the R_{OO} vector. The experimentally measured and computationally predicted values for the geometry of the water dimer can be found in Table V. Also in Table V, we see the geometry parameters computed at 0.1 K for the TIP4P/Ice and TIP1P/Ice models.

	R_{OO} (Å)	θ (°)	ϕ (°)
Expt.	2.95	51 ± 10	57 ± 10
Ab initio	2.91	56	58
TIP4P/Ice	2.79	52.52	43.17
TIP1P/Ice	2.83	40.56	36.59

TABLE V: Geometric parameters of the TIP4P/Ice and TIP1P/Ice gas phase water dimer. Ab initio and Expt. values were taken from another source[7].

Testing Electrostatic Cutoff

First we will see if we can recover the TIP4P/Ice dimer geometry by decreasing damping α to 0.05 Å^{-1} and vary the cutoff radius for the electrostatics. In Figure 4, we see that with very small damping α, increasing the cutoff radius of the potential does not recover the TIP4P/Ice calculated geometry.

Varying Lennard-Jones Parameters

In our initial test, as seen in Figure 5, the Lennard-Jones parameter σ was varied while holding the other parameters of the TIP1P/Ice model constant. We see that the ab. initio predicted R_{OO} separation distance of 2.91 Åis obtained when σ is set to approximately 3.25 Å. However, the two angles θ and ϕ tend to decrease with increasing values of σ, and result in values of about 36°and 31°, which is in poor agreement with the ab. initio calculations. Also, changing the Lennard-Jones parameter σ will drastically alter the condensed phase properties of the model. Namely, the radial distribution function is very sensative to σ. The location of the first solvation shell can be tuned by σ, so we will initially retain the TIP4P/Ice model's value of 3.1668 Å and vary it later if the radial distribution function is off.

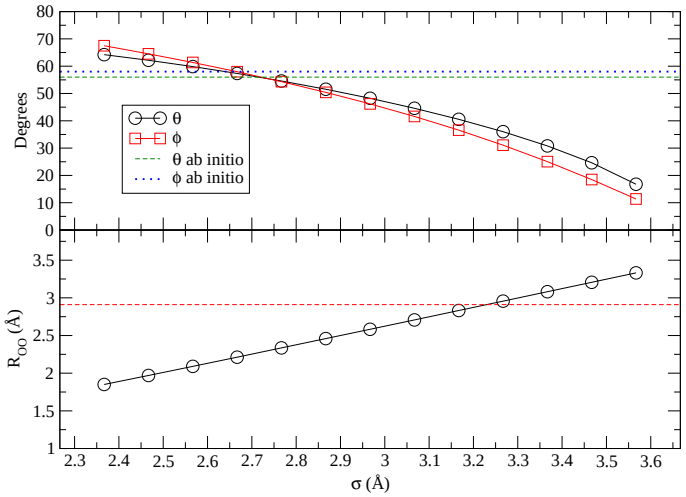

FIG. 5: The Lennard-Jones parameter σ was varied while holding the other parameters of the TIP1P/Ice model constant.

Next, we will vary the Lennard-Jones parameter ϵ, as seen in Figure 6. We see that the ab. initio calculated value of R_{OO} distance of about 2.91 Åis achieved when ϵ is set to approximately 0.275 kcal/mol. However, both θ and ϕ tend to decrease with increasing ϵ, and the resulting values for the two angles at this value of ϵ are approximately 38°and 33°, which are again far from the predicted values. Changing ϵ is not a great way to pa-

rameterize the model though, and we will avoid doing so as much as possible.

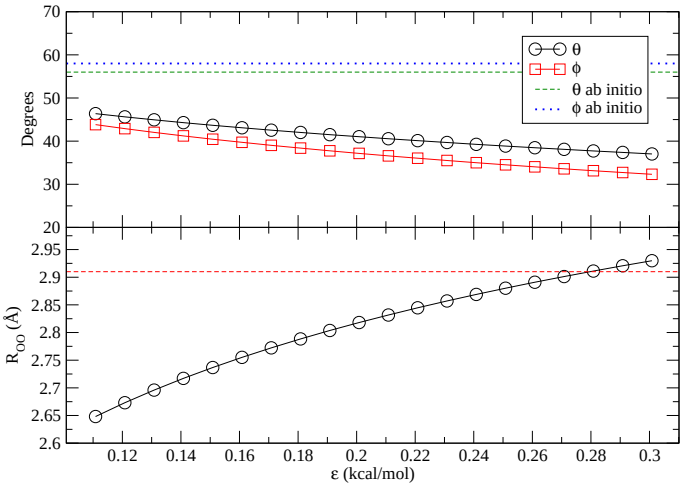

FIG. 6: The Lennard-Jones parameter ϵ was varied while holding the other parameters of the TIP1P/Ice model constant.

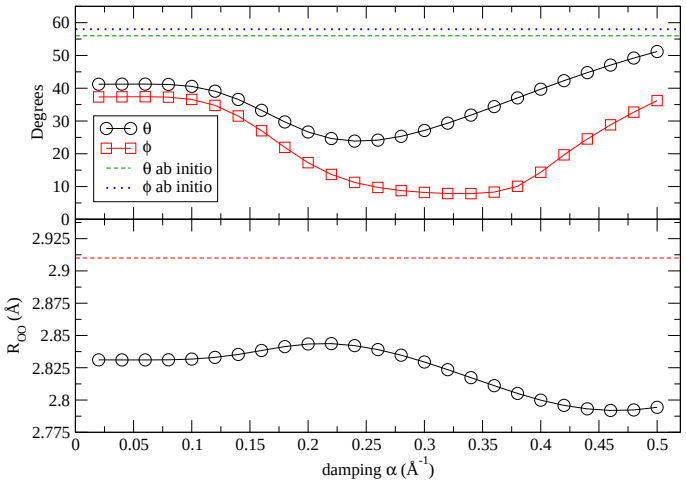

FIG. 7: Damping α was varied while holding the otherparameters of the TIP1P/Ice model constant.

Varying Damping α

Having changed both the Lennard-Jones parameters independently and not achieving the desired values for the separation distance or angles of the gas phase water dimer, the next natural parameter of the TIP1P/Ice model to vary would be the dipole or quadrupole moment. Before doing so, however, we will vary the damping α value which effects how the electrostatics are calculated in OpenMD[8]. In Figure 7, we see that R_{OO} is minimally effected by varying damping α for small values of α. For values larger than about 0.25 $Å^{-1}$, the dimer separation distance decreases slighty. However, the ab. initio calculated distance is not recovered by varying damping α alone. The angles θ and ϕ also do not converge on the ab. initio predicted values over the range of damping α investigated here. After talking with Madan, damping α values of about 0.1 $Å^{-1}$ are suitable for handling the calculation of dipoles and quadrupoles, which is the value that has been used in all other Tests shown here.

Varing the Quadrupole: Introduction of Q_{xx}

A possible reason we have not been able to capture the correct gas phase water dimer geometry by modifying the Lennard-Jones parameters, may be due to the initial construction of the quadrupole tensor for the TIP1P/Ice model. In this model, as with all planar water models, one of the quadrupole tensor's main diagonal elements will be zero, given intelligent choice of origin for the coordinate system. In our construction, this is the Q_{xx} term, as seen in Table IV. In the following Tests, we will try to incorporate the quadrupole moment of the x-dimension into our model.

We will consider varying the quadrupole tensor elements of the TIP1P/Ice model while holding all other parameters constant. This requires special consideration though, as we may not want to deviate from TIP1P/Ice's Q_T or TrQ initial values. We initially will consider a Test in which Q_T is conserved while varying Q_{xx} by the following constraints.

$$Q'_{yy} = Q_{yy} + \lambda \tag{8}$$

$$Q'_{xx} = Q_{xx} - \lambda \tag{9}$$

While Q_T is conserved in this Test, TrQ is not. In Test 4, seen in Figure 8, a similar behavior is apparent as we vary the value of Q_{xx}. Here the TrQ is not conserved, and we have plotted the same data from Figure 8 by the TrQ in Figure 9. In both graphs, However, the angle ϕ is larger than θ at negative values of Q_{xx} here while θ was larger than ϕ when we varied Q_{zz}. Again no value of Q_{xx} results in the R_{OO} separation predicted by the ab initio calculations. The angles also cross over one another as seen previously.

In the next Test, we allow Q_{xx} to vary as in the previous Test, however we now change Q_{zz} in such a way to keep the TrQ constant to it's initial value, as well as varying Q_{yy} in order to conserve Q_T. In Figure 10, we see that the dimer separation distance R_{OO} peaks at a Q_{xx} value of about -0.1 DÅ , and the angles have the right ordering for which is larger at this value. However, neither the R_{OO} or the angles are the correct numerical values as predicted by the ab initio calculations. Therefore, we will increase the value of σ to 3.2668 Å , determined by

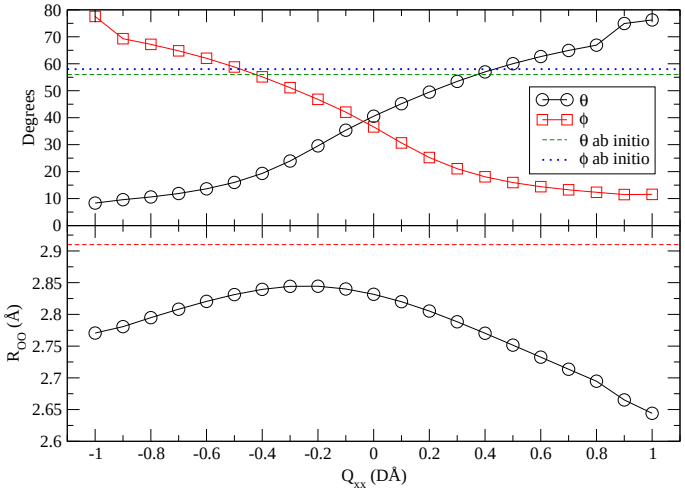

FIG. 8: The Q_{xx} components of the traced quadrupole tensor were varied while simultaneously adjusting the Q_{yy} component such that the Q_T value for the TIP1P/Ice model was held constant. All other parameters were also held constant and equal to the TIP1P/Ice parameters during this test.This means that $Tr(Q)$ varied since the Q_{zz} component was not adjusted asQ_{xx} was varied.

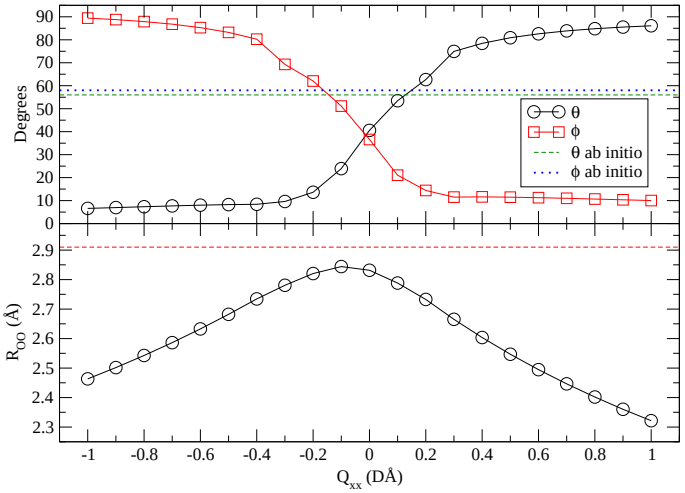

FIG. 10: The Q_{xx} components of the traced quadrupole tensor were varied while simultaneously adjusting the Q_{yy} component such that the Q_T value for the TIP1P/Ice model was held constant. The Q_{zz} component of the quadrupole tensor was also varied in such a way as to keep the $Tr(Q)$ held constant to the TIP1P/Ice value. We see here that the angles cross overone another as in Figure 8.

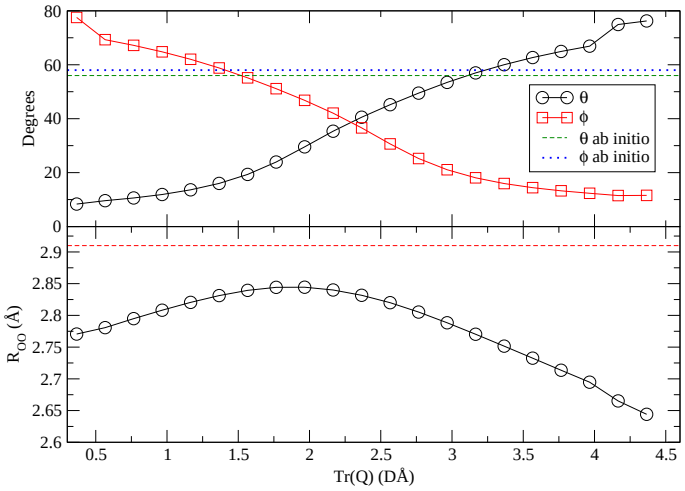

FIG. 9: The same data as plotted in Figure 8, nowplotted as a function of the TrQ.

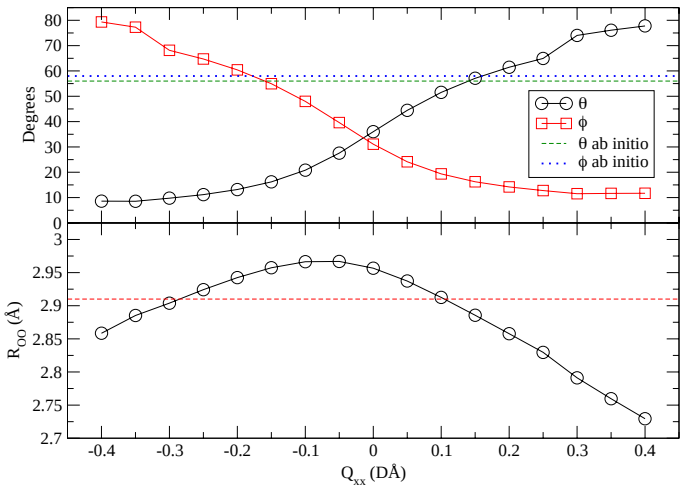

FIG. 11: Setting σ to 3.2668 Å , vary Q_{xx} while simultanesouly adjusting Q_{yy} and Q_{zz} to conserve Q_T and TrQ.

the R_{OO} distance in Figure 5. The results of doing so are shown in Figure 11. Here we see that we have overshot the value of R_{OO}, and that our range of values of Q_{xx} is still quite large. Thus in the next Test, shown in Figure 12, we have adapted a σ value of 3.2268 Å . Here we see that we can accurately achieve the correct ordering of the angles, and approximately the correct value for R_{OO} at Q_{xx} values of about -0.02 DÅ .

It appears that we have achieved as close to the ab initio predicted values as possbile without changing some of our fundamental assumptions. From Figure 12, I believe that by scaling the quadrupole and dipole by the same constant, thus keeping their ratio the same, we may be able to achieve closer agreement with the ab initio predictions. While Abascal and Vega believe that the largest value of Q_T that will give reasonable T_m for ice I_h to be approximately 2.56 DÅ , this prediction is made from water models which contain point charges located on the Hydrogens. These charges cause a torque on the other water molecule in the dimer structure, resulting in a change of the magnitude of the angles.

In the following Test, Q_{xx} was varied while simultaneously varying Q_{yy} to conserve the value of Q_T. μ was also scaled by $\mu = 0.996 Q_T$ for each Q_T investigated. The TrQ was set to 2.365707 DÅ , and σ was set to

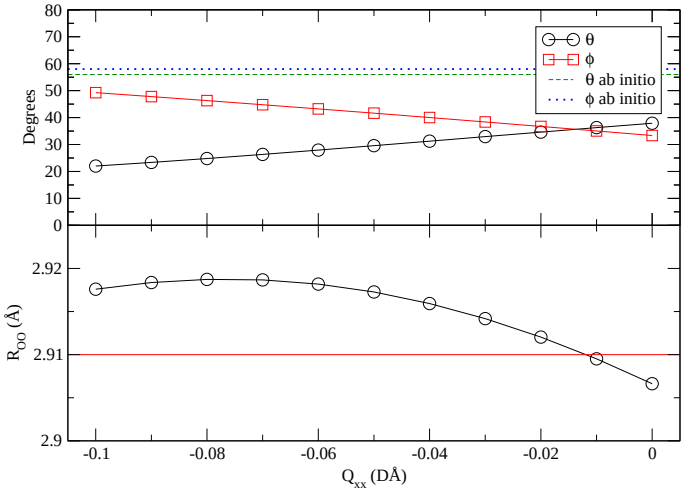

FIG. 12: Setting σ to 3.2268 Å , vary Q_{xx} while simultaneously adjusting Q_{yy} and Qzz to conserve Q_T and TrQ.

3.2268 Å . In Figure 13,R_{OO}, θ, and ϕ are shown as Q_{xx} and Q_{yy} are varied.

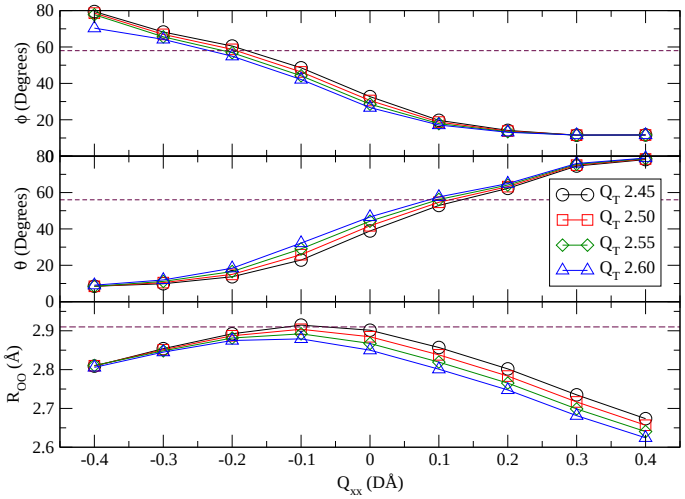

FIG. 13: Here Q_{xx} and Q_{yy} are varied simulatneously to conserve the value of Q_T. μ is scaled as $0.996Q_T$, thus the ratio of μ to Q_T is conserved for each Test of Q_T. The TrQ is fixed to a set value, thus Q_{zz} varies as the other components do.

In the next Test, the dipole moment of the model was varied by some scalar amount (λ), relative to the Q_T chosen. The Q_{xx} component of the quadrupole tensor was set to null, so Q_{yy} varied for each case of Q_T. Q_{zz} was fixed to the TIP1P/Ice model's value. The results of this test can be seen in Figure 14.

In the next section, I will construct a water model similar to the TIP1P/Ice model, however, it will not be the result of collapsing a many-site model onto a single-site. This model will be derived from the results shown in this section with a larger dipole and quadrupole, in attempts

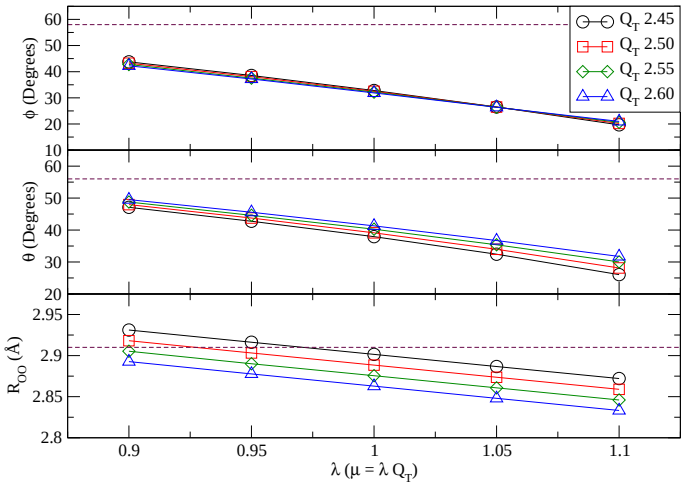

FIG. 14

to increase the magnitude of both of the angles without obscuring their ordering or the R_{OO} values obtained above.

TIP1P/Ice 2.0

In this section, we will worry less about holding Q_T constant, and instead hold QBar constant. In Figure 15, we have the results of varying Q_{yy} while holding Q_{xx} constant at 0.1 DÅ , and varying Q_{zz} such that QBar fixed at the TIP4P/Ice value. However, we see that we do not recover the TIP4P/Ice water dimer geometry.

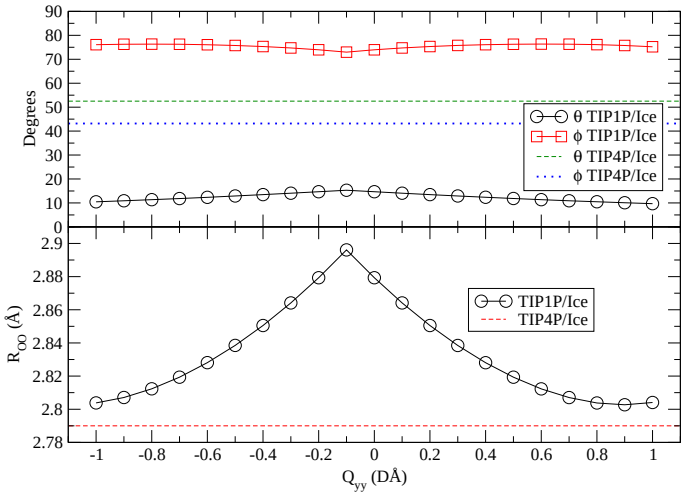

FIG. 15: $Q_{xx} = -0.1$, QBar set to the TIP4P/Ice QBar value of 2.8141, Q_{zz} was modified to keep this constant as Q_{yy} changed.

It is interesting to note that the value of ϕ in Figure 15 is much greater than initially expected from Figure 8. There, we would predict $\phi \approx 40$ degrees, while here we have obtained a value of about 76 degrees. Also, there

does not appear to be any appreciable change in the values of θ as we vary Q_{yy}. This makes me wonder what controls the value of θ, as it appears to not be the value of Q_{yy} as initially thought. In Figure 16, we have held Q_{yy} constant at -0.1 DÅ , and varied Q_{xx} to see if it controls both ϕ and θ.

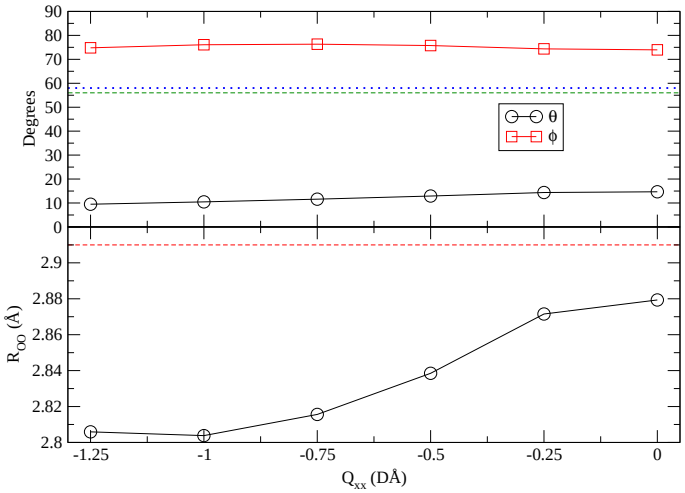

FIG. 16: $Q_{yy} = -0.1$, Q_{zz} was varied to keep QBar constant and equal to the TIP4P/Ice model's value of 2.8141.

From Figure 16, we see that while R_{OO} is slightly sensative to the value of Q_{xx}, the angles θ and ϕ are both insensative to it. In order to try and understand if and how the angles are dependent on QBar, I have re-plotted the data from Figure 10 as a function of QBar instead of Q_{xx}. This can be seen in Figure 17.

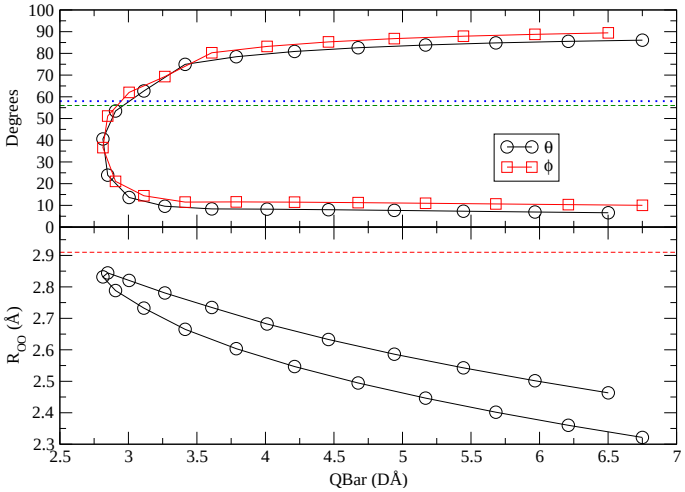

FIG. 17: Q_{xx} and Q_{yy} varied while holding Q_T constant, Q_{zz} varied in order to keep TrQ constant. Both Q_T and TrQ were set to the TIP4P/Ice model value.

An interesting follow up test will be to set Q_{xx} and Q_{yy} to -0.1, Q_{zz} to 1.3071, and vary μ to see if the desired angles can be achieved with a smaller dipole moment. The results of doing so are shown in Figure 18.

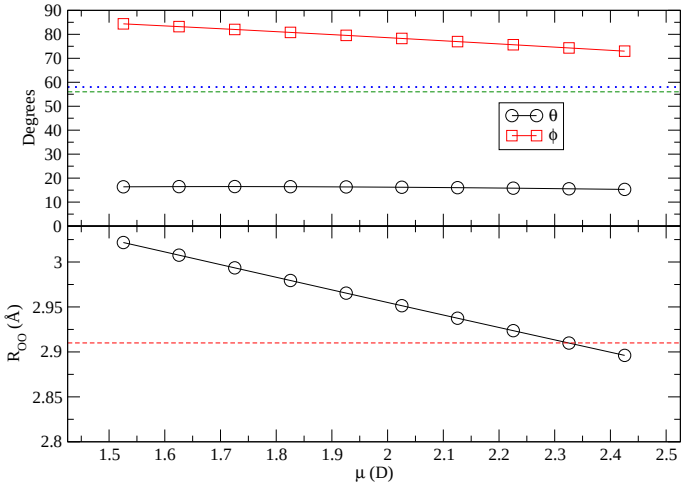

FIG. 18: $Q_{xx} = -0.1$, $Q_{yy} = -0.1$, $Q_{zz} = 1.3701$ which ensures QBar is set to the TIP4P/Ice model value of 2.8141 DÅ .

In Figure 18, we see that as we decrease the value of the dipole moment, the water dimer's separation distance, R_{OO} gradually becomes larger. The angle ϕ increases slightly with decreasing μ, however, θ is relatively insensitive to the value of μ.

In the next Test, we have set the Lennard-Jones parameters to that of the TIP4P/Ice model, as well as the Q_{xx} and Qzz values. Q_{yy} is allowed to vary, and as such, Q_T and QBar both vary. In Figure 19, we see that the angle θ is obtained when Q_{yy} is set to about 1.87 DÅ . However, we see that we miss the dimer separation distance at this value of Q_{yy}, as well as the angle ϕ, which we believe to be the less important of the two angles.

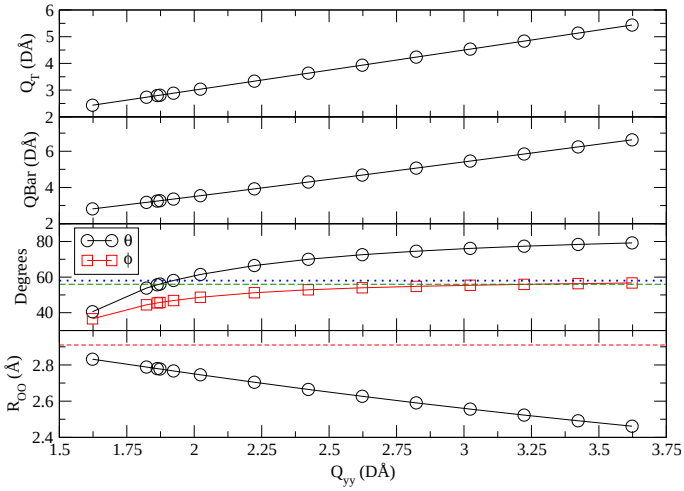

FIG. 19: Q_{xx} and Q_{zz} are set to the TIP4P/Ice value, as well as the Lennard-Jones parameters.The left most data point is the parameter set of the TIP4P/Ice model.

In a similar way, we have held Q_{yy} and Q_{zz} constant while varying Q_{xx}. The results of doing so can be seen in Figure 20.

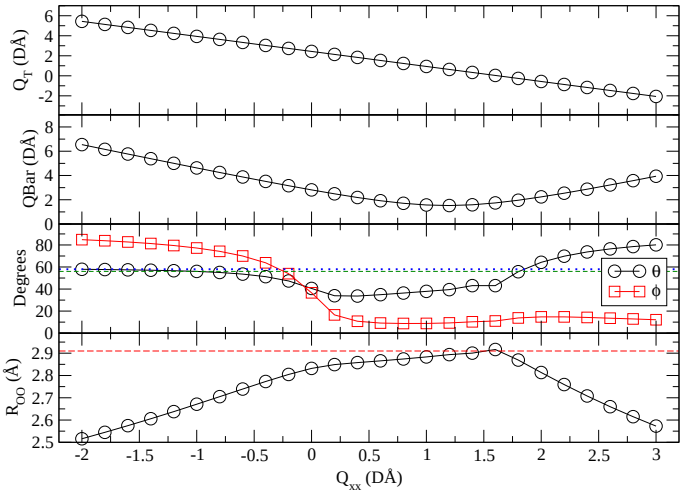

FIG. 20: Q_{yy} and Q_{zz} are set to the TIP4P/Ice value,as well as the Lennard-Jones parameters.The left most data point is the parameter set of the TIP4P/Ice model.

Finally, we have finished the permutation by varying Q_{zz} while holding Q_{xx} and Qyy constant at their original TIP4P/Ice values, as seen in Figure 21.

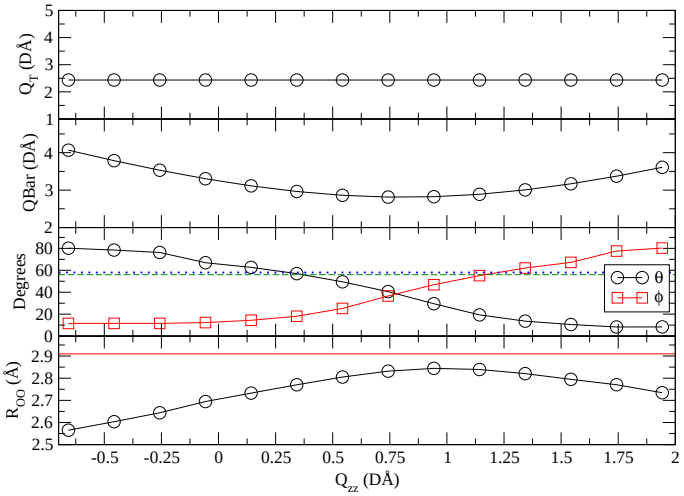

FIG. 21: Q_{xx} and Q_{yy} are set to the TIP4P/Ice value, as well as the Lennard-Jones parameters.The left most data point is the parameter set of the TIP4P/Ice model.

Bulk Properties

As an initial test of the bulk phase properties, I have equilibrated two separate water boxes, one containing 1372 molecules, and one containing 4000 molecules. The resulting geometry was a cubic box with side length of 48.57617 Å . The molecules were propaged at 300K for 1 nanosecond, saving coordinates every 0.1 ps for analysis. The three-dimensional diffusion constant was found to be $5.488 \times 10^{-5}\mathrm{cm}^2\mathrm{s}^{-1}$. This is about a factor of two larger than the experimentally reported value of 2.30 $\mathrm{cm}^2\mathrm{s}^{-1}$. We attribute this difference to a lack of strength of hydrogen bonding. Due to this, we will try playing with the dipole strength and the Q_{zz} values.

Basal Ice I_h/water Coexistence

In order to tune the model to the desired observable, I have begun testing the model at the ice I_h/water interface, exposing a basal plane to bulk water. This system was prepared by constructing a large block of ice from crystallographic coordinates taken from Hirsch and Ojamae structure number 6[**?**]. The constructed block is periodic in all three dimensions. The block was positioned in a simulation cell such that the basal face pointed along the positive z-dimension. The ice block was allowed to relax and equilibrated to 75 K. Separately, a simulation box of liquid water with a density of 0.999 g cm^{-1} was equilibrated to 75 K, with equivalent x and y dimensions to the ice block, and twice that in z. The ice block was then merged with the liquid system by carving out any liquid water molecule within three angstroms of a molecule from the ice system.

CONCLUSIONS

In conclusion, we have not yet found an accurate model.

[1] J. L. F. Abascal and C. Vega, *Phys. Rev. Lett.* **98**, 237801 (2007).

[2] J. L. F. Abascal*, , and C. Vega, *The Journal of Physical Chemistry C* **111**, 15811 (2007).

[3] J. L. F. Abascal and C. Vega, *Phys. Chem. Chem. Phys.* **9**, 2775 (2007).

[4] S. L. Carnie and G. N. Patey, *Mol. Phys.* **47**, 1129 (1982).

[5] S. W. Rick, *J. Chem. Phys.* **120**, 6085 (2004).

[6] J. L. F. Abascal, E. Sanz, R. Garcia Fernandec, and C. Vega, *J. Chem. Phys.* **122**, 234511 (2005).

[7] H. Yu and W. F. can Gunsteren, *J. Chem. Phys.* **121**, 9549 (2004).

[8] J. D. Gezelter et al., OpenMD, an Open Source Engine for Molecular Dynamics, Available at `http://openmd.org`, 2014.